Volume 10 | Issue 3 | December 2020 ISSN 2182-0287

Journal of Integrated OMICS

a methodological journal

JIOMICS

Journal of Integrated OMICS

Focus and Scope

Journal of Integrated OMICS, JIOMICS, provides a forum for the publication of original research papers, preliminary communications, technical notes and critical reviews in all branches of pure and applied "-omics", such as genomics, proteomics, lipidomics, metabolomics or metallomics. The manuscripts must address methodological development. Contributions are evaluated based on established guidelines, including the fundamental nature of the study, scientific novelty, and substantial improvement or advantage over existing technology or method. Original research papers on fundamental studies, and novel sensor and instrumentation development, are especially encouraged. It is expected that improvements will also be demonstrated within the context of (or with regard to) a specific biological question; ability to promote the analysis of molecular mechanisms is of particular interest. Novel or improved applications in areas such as clinical, medicinal and biological chemistry, environmental analysis, pharmacology and materials science and engineering are welcome.

AUSTRALIA AND NEW ZEALAND

EUROPE

JOURNAL OF INTEGRATED OMICS

A methodological Journal

SPECIAL ISSUE: SELECTED ABSTRACTS OF THE III INTERNATIONAL CAPARICA CONFERENCE IN SPLICING 2020

ORIGINAL ARTICLES

SPECIAL ISSUE

SELECTED ABSTRACTS OF THE III INTERNATIONAL CAPARICA CONFERENCE IN SPLICING 2020

JOURNAL OF INTEGRATED OMICS
A METHODOLOGICAL JOURNAL
HTTP://WWW.JIOMICS.COM

SPECIAL ISSUE: SELECTED ABSTRACTS OF THE III INTERNATIONAL CAPARICA CONFERENCE IN SPLICING (SPLICING 2020)

c-Jun and RBM39 co-regulate alternative splicing induced by chemotherapy compounds

F. Chakrama[1,4], F. Lemaitre[1], F. Dequiedt[1], B. Chabot[2], R. Klinck[2], A. Colige[3], J. Piette[4], C. Lambert[3] and Y. Habraken[1,4*]

[1]Gene Expression and Cancer, GIGA-Molecular Biology of Diseases, University of Liège, BE; [2]Laboratory of Functional Genomics and Department of Microbiology and Infectiology, Faculty of Medicine and Health Sciences, University of Sherbrooke, Sherbrooke, Québec, CA; [3]Laboratory of Connective Tissues Biology, Giga-Cancer, University of Liège, BE; [4]Laboratory of Virology and Immunology, GIGA-Molecular Biology of Diseases, University of Liège, BE

Available Online: 31 December 2020

ABSTRACT

By generating multiple messenger RNAs from a single gene, alternative splicing (AS) controls and enlarges the diversity of the transcriptome. In human cells, 90% of the genes can undergo alternative splicing making this mechanism a general process. AS participates to stress responses as it allows a rapid modification of the transcriptome. In this work, we are investigating the global regulation of splicing following chemotherapy.

Previously, we performed a NGS sequencing of MCF7 cells treated by cisplatin and reported the modifications of both mRNA steady state levels and splicing. We began to study the molecular mechanism leading to spliceosome control after addition of cisplatin and demonstrated the importance of SRSF4 (1).

In this work, we selected a strong cisplatin-induced exon skipping event and used it as reporter to investigate the molecular regulation of the spliceosome by cisplatin. First, an siRNA screening targeting 57 RNA binding proteins was conducted. It was noted that the depletion of SF3A1, SF3B4, U2AF1 and RBM39 induced AS similar to cisplatin while the depletion of others was neutral or prevented it. Since cisplatin did not reduce the level of these 4 proteins, the AS regulation resided elsewhere. Second, as RBM39 was shown to interact with c-Jun by GST pull-down and yeast 2 hybrid(2), we investigated this interaction by immunoprecipitation and NanoLuc 2 hybrid in our experimental settings and determined that the interaction was cisplatin-dependent and RNA- and DNA-independent. Interestingly, while the depletion of RBM39 favored the studied skipping event, the depletion of c-Jun prevented it. The presence of RBM39 on the transcript intron adjacent to the skipped exon was confirmed by RNA immunoprecipitation. To investigate the role of c-Jun and RBM39 in AS on a global scale, we repeated the transcriptome analysis of MCF7 cells depleted in RBM39 and c-Jun, treated or not with cisplatin, and compared their transcriptomes.

Acknowledgments:

This work was supported by founds from ULiège, ARC, Télévie, the Belgian F.R.S.-FNRS, European cofunds, and Fonds Léon Frédéricq.

References:

[1] Gabriel M, Delforge Y, Deward A, Habraken Y, Hennuy B, Piette J, Klinck R, Chabot B, Colige A, Lambert C. BMC Cancer 15 (2015) 227.

[2] Jung D, Na S, Na D, Lee J. J Biol Chem. 277 (2002) 1229-1234.

Correspondence: Email - yvettte.habraken@uliege.be

JOURNAL OF INTEGRATED OMICS
A METHODOLOGICAL JOURNAL
HTTP://WWW.JIOMICS.COM

SPECIAL ISSUE: SELECTED ABSTRACTS OF THE III INTERNATIONAL CAPARICA CONFERENCE IN SPLICING (SPLICING 2020)

hnRNPA1 promotes cancer progression in response to FGF2 signalling

Olivier E Pardo[1]*, Rajat Roy[1], Yueyang Huang[1], Filippo Prischi[2], J Mark Skehel[3], Michael J Secl[1]

[1]Division of Cancer, Department of Surgery and Cancer, Imperial College, London, UK; [2]School of Biological Sciences, University of Essex, Colchester, UK; [3]Biological Mass Spectrometry and Proteomics, MRC LMB, Cambridge, UK

Available Online: 31 December 2020

ABSTRACT

Increase in cap-independent translation of antiapoptotic proteins, such as BCL-XL and XIAP, is involved in the development of drug resistance in cancer. We previously demonstrated the role of Fibroblast Growth Factor 2 (FGF2) signalling and S6 kinase 2 (S6K2) activity in this process 1, but the downstream mediator(s) of this translational response remained unknown. We used tandem affinity purification using S6K2 as bait as well as quantitative phospho-proteomics in the presence and absence of FGF2 stimulation in small cell lung cancer and HEK 293 cells to identify new S6K2 interactors and downstream mediators of the FGF2 pathway. We showed that S6K2 interacts with and phosphorylates the heteronuclear ribonuclear protein, hnRNPA1, on Ser 4 and 6 2. This increases the association of this protein with BCLXL and XIAP mRNAs to promote their nuclear export while de-repressing their translation. A nonphosphorylatible S4/6A hnRNPA1 mutant prevented this process from occurring and impaired the prosurvival activity of FGF2/S6K2 signalling. Following phosphorylation and transfer to the cytoplasm in complex with mRNAs, phospho-hnRNPA1 associates with 14-3-3 to be sumoylated on K189 within a multi-protein complex involving UBC9. This targets hnRNPA1 for re-import into the nucleus in a caryopherin-dependent manner, a step that is essential for translational derepression of target mRNAs. The importance of this pathway for the translation of BCL-XL and XIAP in vivo was suggested by immunohistochemical staining of lung cancer tissue microarrays showing that increased S6K2 expression correlated with decreased cytoplasmic hnRNPA1 and increased BCL-XL levels. We subsequently wanted to determine large-scale changes in hnRNPA1/mRNA binding that occur in response to FGF2 and performed an RNA-IP coupled to RNA-Seq. Analysis of the interactome changes revealed several biological processes controlled by hnRNPA1 in response to FGF2, including several inflammatory pathways. In particular, this revealed the involvement of hnRNPA1 in regulating IFNγ response, with hnRNPA1 downregulation leading to sensitisation of sarcoma cells to this cytokine. We therefore initiated a drug discovery project to identify hnRNPA1 inhibitors and performed an X-Chem screen that revealed several chemical fragments specifically binding to areas of functional significance to hnRNPA1 biological activity. In conclusion, hnRNPA1 signalling promotes cancer progression and small-molecule inhibitors that hinder the activity of this protein may provide new tools to target various types of cancer.

Acknowledgments:

We would like to thank the Clement-Wheeler trust, the European Union FP7 program (LungTarget consortium) and the Cancer Treatment and Research Trust (CTRT) for financial support towards this research. Also, we gratefully acknowledge infrastructure support from the Cancer Research UK Imperial Centre, the Imperial Experimental Cancer Medicine Centre and the National Institute for Health Research Imperial Biomedical Research Centre.

References:

[1] Pardo, O. E. et al. The EMBO journal 25, (2006), 3078-3088,.
[2] Roy, R. et al. Nucleic Acids Res 42, (2014), 12483-12497,.

Correspondence: Email - o.pardo@imperial.ac.uk

JOURNAL OF INTEGRATED OMICS
A METHODOLOGICAL JOURNAL
HTTP://WWW.JIOMICS.COM

SPECIAL ISSUE: SELECTED ABSTRACTS OF THE III INTERNATIONAL CAPARICA CONFERENCE IN SPLICING (SPLICING 2020)

Muscleblind-like 2 controls the hypoxia response of cancer cells

Sandra Fischer[1], Antonella Di Liddo[2], Katarzyna Taylor[3], Jamina S. Gerhardus[1], Krzysztof Sobczak[3], Kathi Zarnack[2] and Julia E. Weigand[1]*

[1]Department of Biology, Technische Universität Darmstadt, Darmstadt, 64287, Germany; [2]Buchmann Institute for Molecular Life Sciences, Goethe University Frankfurt, Frankfurt am Main, 60438, Germany; [3]Department of Gene Expression, Institute of Molecular Biology and Biotechnology, Faculty of Biology, Adam Mickiewicz University, Poznan, 61-614, Poland

Available Online: 31 December 2020

ABSTRACT

Hypoxia is a common feature in solid tumors as the rapidly proliferating tumor cells outgrow their blood supply. Gene expression changes in response to hypoxia add to the genetic instability of cancer cells and promote invasion and metastasis. Thus, tumor hypoxia is an indicator of more aggressive tumors and poor patient prognosis. Moreover, tumor hypoxia counteracts radio-, chemo- and immunotherapy, highlighting the importance of developing therapies effective in oxygen depleted conditions. On top of the well-studied transcriptional response exerted by the hypoxia inducible factor (HIF) family of transcription factors, hypoxia has a major effect on alternative splicing and the expression of splicing factors.

Comparison of the transcriptomic changes in response to chronic hypoxia of lung and breast cancer cells showed highly concordant changes in transcript abundance, but divergent, cell type-specific changes in alternative splicing. The levels of splicing factors are predominantly reduced in response to chronic hypoxia. One specifically induced splicing factor is muscle-blind like 2 (MBNL2), known as a regulator of tissue-specific alternative splicing. Transcriptomic changes after knockdown of MBNL2 in hypoxic cancer cells show that it promotes adaptation to hypoxia by increasing HIF response genes, such as VEGFA, at the mRNA and protein level. In addition, MBNL2 reverses hypoxia-dependent changes in alternative splicing. Consistent with its contribution to hypoxia adaptation, MBNL2 promotes cell viability and migration of hypoxic cancer cells. In summary, MBNL2 positively contributes to cancer progression through the activation of hypoxia response genes.

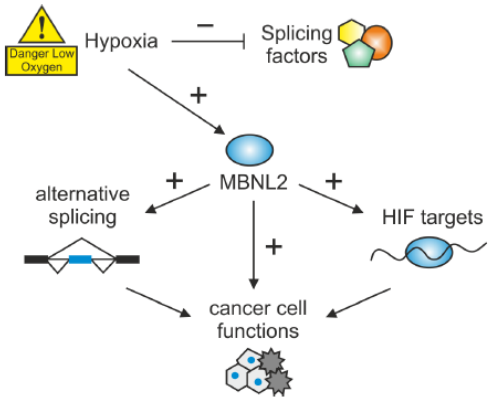

Figure 1 | MBNL2 governs the adaptation of cancer cells to hypoxia

Correspondence: Email - julia.weigand@tu-darmstadt.de

JOURNAL OF INTEGRATED OMICS
A METHODOLOGICAL JOURNAL
HTTP://WWW.JIOMICS.COM

SPECIAL ISSUE: SELECTED ABSTRACTS OF THE III INTERNATIONAL CAPARICA CONFERENCE IN SPLICING (SPLICING 2020)

Expression of proline-rich proteins, P-B1, P-B, and BPLP, the parent proteins of opiorphin family, in human saliva

Eiichi Saitoh[1]*, Akihito Ochiai[2], Takaaki Tanaka[2], Masayuki Taniguchi[2], Tetsuo Kato[3], Akane Imai[4], Satoko Isemura[4]

[1]Niigata Institute of Technology; [2]Niigata University; [3]Tokyo Dental College; [4]The Nippon Dental University College at Niigata, Japan

Available Online: 31 December 2020

ABSTRACT

The NCBI data base demonstrated that multiple transcripts of the genes, OPRPN (alias PROL1) coding for the precursor of basic proline-rich lacrimal protein BPLP (UniProt/Swiss-Prot, Q99935, 248 amino acids) [1], PBI (alias SMR3A or PROL5) for the precursor of P-B1 (Q99954, 134 a. a.) and PBII (alias SMR3B or PROL3) for the precursor of P-B (P02814, 79 a. a.) on chromosome 4q13.3 are synthesized by alternative splicing, as shown in Fig. 1. The mRNA (NCBI, AK312075) and two mRNAs (BC144529 and BC015327) code for the precursor of P-B1 and P-B, respectively. Recently, we have identified the P-B variant (Q504X8, 106 a. a.) encoded by BC094707-mRNA [2]. The three proteins are carrying an identical signal peptide of 22 a. a., an opiorphin-homolog (QRGPR), and an anti-breast cancer peptide (RGPYPPGPLAPP). In case of the OPRPN gene, the mRNA (NM_021225.5) for BPLP and the mRNA (Genbank, S83198.1/HC924356.1) for a homolog of BPLP (201 a. a.) are stored in the database. BPLP and BPLP-homolog share the signal peptide and the N-terminal 144 a. a. sequence, and the both are carrying opiorphin (QRFSR) having a painkilling effect. In addition, the mRNA (NM_001302807.2) for a nonproline- rich protein (127 a. a.) without opiorphin can also be found in the data base. At present, BPLP is known to be expressed in exosome II of human whole saliva, tears, submandibular-sublingual saliva, and parotid saliva by MALDI-TOF-MS. In this study, we further analyzed multiple fragments separated from the tryptic digest of human salivary proteins fractionated by two-dimensional chromatography. As the result, two tryptic fragments (-21MK-LTFFGLLALISCFTPSESQ+2R and -20KLTFFGLLALISCFTPSESQ+2R) covering the signal peptides of BPLP and BPLP-homolog including the fragment (+22WVPPSPPPPYDSRLNSPLSLPFVPG+48R) covering the sequence near the N-termini of the both. Surprisingly, the tryptic fragment covering the C-terminal portion of BPLP-homolog (+166ACHLHISSNP+176R) was also detected by MALDI-TOF-MS, suggesting that mRNA for BPLP-homolog is generated by the insertion of "G" between "386G" and "387C" in the fourth exon of the OPRPN gene. Western blot with commercially available anti-PROL1 antibody (Abcam co., Japan) showed two sets of positive signals; one is a set of positive signals raging in 20 -22K, another 25-27K. This suggests the possibility that microheterogeneity due to N-glycosylation occurs in the two proteins. However, the nonproline- rich protein described above and P-B1 could not be identified in the present study. In conclusion, our data demonstrated that BPLP and BPLP-homolog are present in human whole saliva. This finding suggests the possibility that mRNA for BPLP-homolog may be originated from pre-mRNA for BPLP by a mechanism of RNA editing.

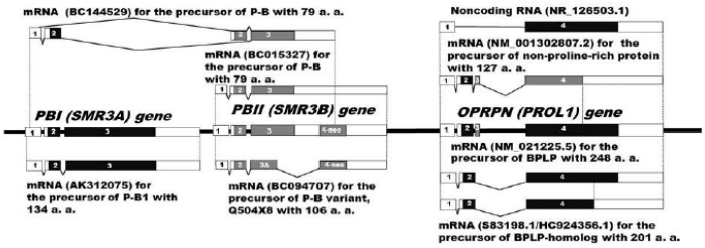

Figure 1 | Summary of alternative splicing of the genes, PBI, PBII, and OPRPN.

References:

[1] D.P. Dickinson, M. Thiesse, Curr. Eye Res. 15 (1996) 377-86.

[2] E. Saitoh, T. Sega, A. Imai, S. Isemura, T. Kato, A. Ochiai, M. Taniguchi, Arch. Oral Biol. 88 (2018) 10-18.

Correspondence: Email - matteored90@gmail.com

ORIGINAL ARTICLES

JOURNAL OF INTEGRATED OMICS
A METHODOLOGICAL JOURNAL
HTTP://WWW.JIOMICS.COM

ARTICLE | DOI: 10.5584/jiomics.v10i3.341

Integrated Omics in salmon skin mucus for determining consequences of chloramine treatment against parasite infestation

Oscar Daniel Rangel-Huerta[1]*, Lada Ivanova[1], Sigurd Hytterød[1], Anders Moen[2], Silvio Uhlig[1], Anders Gjørwad Hagen[3], Kjetil Olstad[4], Christiane Kruse Fæste[1]

[1] Norwegian Veterinary Institute, Toxinology Research Group; P.O. Box 750 Sentrum, 0106 Oslo, Norway; [2] University of Oslo, Department of Biosciences, Problemveien 7, 0315 Oslo, Norway; [3] Norwegian Institute for Water Research, Gaustadalléen 21, 0349 Oslo, Norway; [4] Norwegian Institute for Nature Research, P.O. Box 5685 Torgarden, NO-7485 Trondheim, Norway.

Received: 22 October 2020 **Accepted:** 15 December 2020 **Available Online**: 31 December 2020

ABSTRACT

The monogenean salmon fluke (*Gyrodactylus salaris*) is an important ectoparasitic pathogen of Atlantic salmon (*Salmo salar*) frequently occurring in Norwegian rivers. High infection rates have reduced populations of salmon parr and led to a decline of upstream-swimming adult fish. Thus, finding efficient measures for the eradication of the parasite is a necessity. The treatments that have been successful so far have the disadvantage of killing all aquatic life and require river rehabilitation and repopulation programs. In the search for more selective agents, chlorine at low concentrations has emerged as a suitable candidate, removing the flukes from the salmon without causing notable adverse consequences. However, more data regarding potential health risks are needed before chlorine can be applied for the large-scale disinfection of Norwegian watercourses. In the present study, we have therefore explored potential effects of exposing on-growing salmon to (mono)chloramine, by combined proteomic and metabolomic profiling of the skin mucus composition. The epidermal mucus protects fish against harmful environmental factors and represents a valuable and easily accessible source for monitoring the health status by analyzing excreted proteins and small molecules. We treated fish with 60 µg/L (Cl_{60}) chloramine for 17 days (E17) and kept them for further 21 days (R21) in non-chlorinated water during a recovery period. A control group (Cl_0) followed the same procedure but without chloramine. Skin mucus was obtained before treatment following a 14-day habituation period (H0), at E17 and at R21, following a previously established mucus absorption protocol. The samples were analyzed by proteomic and metabolomic methods using high-resolution mass spectrometry, and data were processed for further statistical modeling. While there were no significant differences between exposed and control salmon at E17, we observed a considerable time-dependent influence on the mucus composition in both Cl_0 and Cl_{60} groups that were attributed to aging. However, the comparison of Cl_0-R21 vs. Cl_{60}-R21 at study end indicated a chloramine-dependent separation of the groups, mostly caused by proteins classifiable into the biological processes "cellular processes" and "metabolic processes". Overall, the observed differences between treated fish and controls were small, showing that the health risk for salmon exposed to chloramine concentrations below 60 µg/L appears to be low.

Keywords: *Atlantic salmon; integrated omics; chloramine; metabolomics; proteomics; skin mucus*

1. Introduction

Salmon fluke (*Gyrodactylus salaris*) is a leech-like freshwater ectoparasite primarily infecting Atlantic salmon (*Salmo salar*) [1]. It possesses a haptor with 16 hooks at the posterior end and feeds mainly on the skin and fins of juvenile fish. The release of digestive enzymes from the pharynx causes large wounds, and infestation with several flukes is mostly deadly [2]. The introduction of the parasite to Norway from imported smolt in the 1970s has led to catastrophic losses in wild salmon populations, which by 2004 were wiped out in 45 Norwegian rivers [3,4].

The dramatic development initiated an extensive *G. salaris* eradication and river rehabilitation program coordinated by the Norwegian Environment Agency [5]. Among the most used chemicals for the treatment of watercourses are the

***Corresponding author:** Oscar Daniel Rangel-Huerta; Toxinology Research Group, Norwegian Veterinary Institute. P.O. Box 750 Sentrum, 0106 Oslo, Norway; Tel.: +47 48646871; email: oscar.daniel.rangel.huerta@vetinst.no

plant toxin rotenone and aluminum sulfate [6]. Both are effective against the parasite but have the disadvantage of killing all aquatic life, including the salmon. Thus, arduous rescue measures such as wild salmon breeding and repopulation of cleared rivers are necessary. The search for more selective chemicals has identified chloramine as a suitable candidate. It is well documented that chlorine can kill pathogens at concentrations of 0.5 to 1 mg/L in water [7]. At the same time, chlorine levels up to 4 mg/L are considered safe in drinking water. Consequently, chlorine compounds are used, e.g., for the disinfection of drinking water, treatment of wastewater, and disinfection of bacteria and algae contaminations. Chlorine in various forms is the world's most commonly used disinfectant, which also has been utilized as an agent in aquaculture [8–10]. Experiments under controlled conditions in a research facility have shown that hypochlorite added to water at low concentrations between 5 to 50 µg/L was able to remove *G. salaris* from on-growing salmon without having any visible adverse effects on the fish [11]. This was confirmed in a subsequent study in river water [12]. When chlorine was added as (mono)chloramine, the duration of the toxic effect increased considerably compared to the addition as sodium hypochlorite [11,13]. Nevertheless, chloramines can be toxic to fish, and several species within the salmon family (*Salmonidae*) have been described as highly sensitive to chlorine [14]. However, there is wide variation in the reported acute toxicity concentrations, with 96 h LC_{50} values ranging from 10 to 132 µg residual chlorine/L, meaning the proportion of added chlorine to the water that is not immediately deactivated [14]. The term covers free chlorine, including gas, hypochlorous acid, and hypochlorite, as well as bound chlorine such as chloramine, which reacts more slowly and stays longer active. Indication of chronic toxicity to chlorine has been found following exposure to residual chlorine levels as low as 3 µg/L for 12 weeks [15].

The observed differences in chlorine toxicities in *G. salaris* and Atlantic salmon have made it a promising candidate for river treatments. Field trials are in preparation, based on experiences from an on-going experiment using tanks with circulating water from the river Glitra with added (mono) chloramine [16]. Young salmon are exposed to different chlorine concentrations for varying exposure periods with the aim to evaluate a potential impact on fish health and welfare by monitoring a number of physiological parameters. In this context, we have explored the applicability of proteomic and metabolomic profiling for biomarkers of exposure.

Novel technologies such as "omics" can provide insight related to the understanding of biological functions and responses to environmental agents in exposed fish [17]. Proteomics deals with the large-scale determination of gene and cellular functions directly at the protein level [18], whereas metabolomics can elucidate systemic perturbations through the analysis of low-molecular-weight metabolites, delivering a snapshot of the actual status of active biological functions [19]. Therefore, the combination of omics-techniques appeared to be a promising tool for the investigation of possible consequences of chloramine treatment on the skin mucus composition of salmon and for the characterization of affected physiological pathways. Both techniques generate massive datasets that combined can deliver in-depth information about biological processes supporting the understanding of systems biology [20,21].

It was thus the aim of the present study to identify changes in the protein and metabolite compositions in the mucus layer of chloramine-exposed salmon directly after the treatment and after a recovery period using an "Integrated Omics" approach, combining proteomics and metabolomics data by chemometrics.

2. Material and Methods

2.1 Salmon husbandry

Two-year-old salmon with average weights of 65 g and lengths of about 17 cm were obtained from the fish breeding station of the Fish Administration of Drammen City and County (DOFA), Norway. The fish were the progeny of wild salmon from the river Lierelva that were hatched and fostered at DOFA in tanks with water from the river Glitra, a tributary of Lierelva. They were fed with Nutra XP (2 mm pellets) extruded salmon feed (Skretting, Stavanger, Norway) with automatic feeders. The wild salmon was unvaccinated and untagged.

The fish were treated in accordance with the Norwegian regulations concerning the care and use of fish in laboratory experimentation. The present study was part of a larger experiment, approved by the Norwegian Animal Research Authority (FOTS-ID 15598), for the elucidation of effects on salmon from the exposure to (mono)chloramine by analyzing physiological parameters in blood, physical effects on gills, fish behavior and possible changes in the composition of the skin mucus layer [16].

2.2 Exposure of salmon to chloramine in river water

The experiment was designed as an open system with continuous water flow from the river Glitra (T = 12.7°C ± 1.3°C). The water was led into a fiberglass tank (V = 230 L) with overflow, ensuring a stable water supply during the trial period. Overflowing water was led further to two mixing tanks (V = 90 L), where chloramine was added to one of them with a peristaltic pump (Watson-Marlow 323S with a 304MC five-channel cassette pump head, Falmouth, UK) within 3.5 min. The chlorinated water was passed on to the exposure tanks (V = 90 L, 4.8-5.2 L/min flow). In parallel, untreated water was used for control fish. The turbidity, conductivity, and temperature of the river water were analyzed daily. Furthermore, temperature and pH were measured in the exposure tanks. Total chlorine was determined every day in the outflow of the mixing tanks,

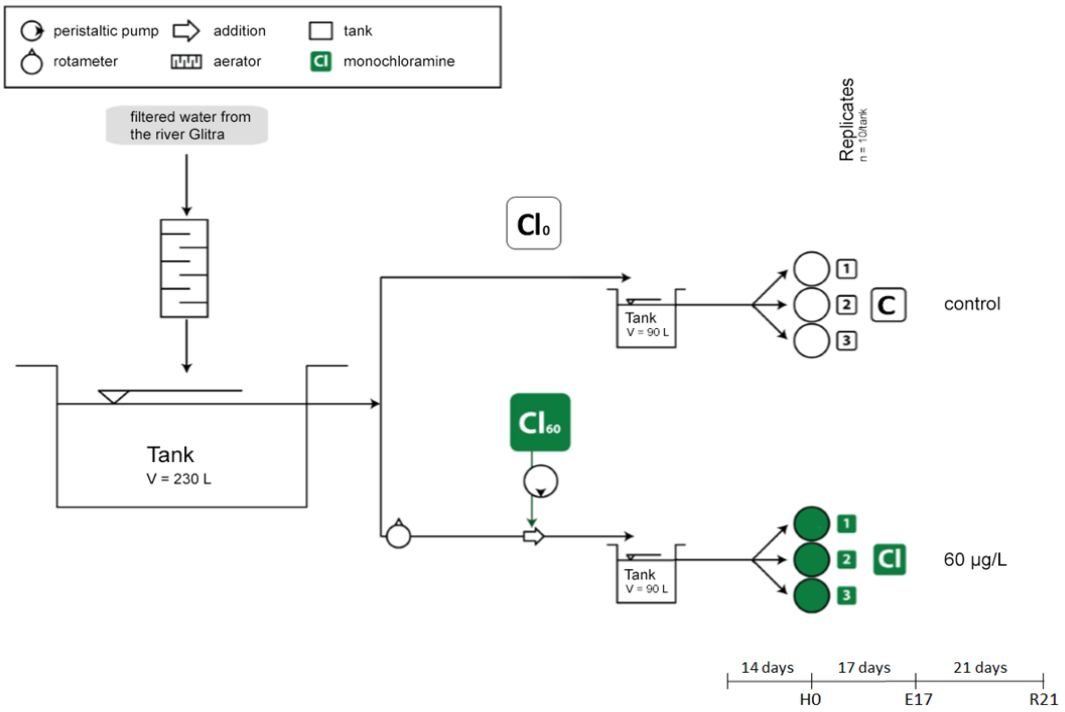

Figure 1 | Flow diagram of the experimental design of the study.

subtracting the background in the non-chlorinated control water.

At the experiment start, the salmon were transferred into the exposure tanks (n=10/tank) and acclimated for two weeks. Three replicate tanks per chloramine-treated fish and corresponding controls were included. The fish were not fed during the study period. After exposure to 60 µg/L (Cl_{60}) chloramine for 17 days, all fish were kept for further 21 days in non-chlorinated water during a recovery period (Figure 1).

2.3 Chloramine dosing scheme

A stock solution containing 400 mg/L (mono)chloramine was prepared by dissolving 5.2 g ammonium chloride in 9 L desalted water, shaking, and the addition of 1 L water containing 23.8 mL concentrated (14 %) hypochlorite solution. The stock solutions were added to the Cl_{60} mixing tanks with 13.5 mL/3.5 min. It was renewed every second day during the first 12 days of the exposure period, and every day during the final five days. The chlorine concentration in the stock solution was analyzed daily in this period because it appeared that it declined faster than expected due to auto-degradation [16]. The actual chlorine level for Cl_{60} was thus about 40 µg/L for the first 12 days of the experiment, while it was adjusted to the nominal values for the last five days.

The concentrations of active chlorine in the exposure tanks were determined as previously described [12]. Briefly, water samples were filtered (0.45 µm pore size), and 25 mL filtrate were blended with 0.15 mL phosphate buffer (0.21 M Na_2HPO_4, 0.34 M KH_2PO_4, 2.7 mM EDTA). Subsequently, N,N-diethyl-p-phenylenediamine sulphate (5.7 mM in 0.7 mM EDTA/0.2 % H_2SO_4) and, after thoroughly mixing, 3 mg solid KI were added. After further mixing, the samples were incubated for 1 h in the dark. Absorption differences to water controls at 510 nm (5 cm optical path) were used (Shimadzu UV1240 mini spectrophotometer, Shimadzu, Kyoto, Japan) to calculate chlorine levels based on a calibration curve of diluted chlorine standards.

2.4 Sampling of salmon skin mucus

Skin mucus was sampled from the fish using a standardized absorption method reported elsewhere [22] in the exposure tanks at the end of a 14-day acclimation period (H0), on day 17 (E17) during chlorine exposure, and on day 21 (R21) in the recovery period (Figure 1). For proteomic analysis, ten fish were included at H0 (n= 10), and two replicates per tank and dose group were used for Cl_0 and Cl_{60} at E17 and R21 (n=6 fish per dose and time point) (Table 1). For the metabolomic analysis, four replicates per tank and dose were obtained for Cl_0 and Cl_{60} at H0, E17, and R21 (n=12 fish per dose and time point) (Table 1).

Skin mucus was sampled after the fish had been killed with a blow to the head. A sterile piece of medical wipe (Kimberly -Clark, Irving, TX, USA) sized 2.5 x 7 cm was placed for about 10 seconds on the left side of the fish behind the gill cover. The wipe was removed, rolled, and transferred into the upper compartment of a Spin-X® polypropylene centrifuge tube (0.22 µm cellulose acetate, Costar, Corning, NY, USA) and stored on ice until centrifugation for 10 min

Table 1 | Sampling plan for proteomic and metabolomic analysis of salmon skin mucus.
#Habituation period: 3 (P) +1 or 4 (M) fish from each replicate tank (n=3); &Exposure period day 17: 2 (P) or 4 (M) fish from each replicate tank (n=3); ¤Recovery period day 21: 2 (P) or 4 (M) fish from each replicate tank (n=3) .

Analysis	H0#	E17&		R21¤		Sum
		Cl_0	Cl_{60}	Cl_0	Cl_{60}	
Proteomics (P)	10	6	6	6	6	34
Metabolomics (M)	12	12	12	12	12	60

with 500 × g at 4 °C. The extracted mucosal fluid was stored at −80°C until further use.

2.5 Determination of protein concentrations

The total protein amount in the mucus fluid samples was determined by applying the Lowry assay (DC Protein Assay, Bio-Rad, Hercules, CA, USA). The samples were measured diluted 1:2 with phosphate-buffered saline (PBS) (pH 7.4), and the mean protein concentrations were calculated from all measured values falling into the calibration curve, ranging from 0.1–1 mg/mL bovine serum albumin (BSA) in PBS.

2.6 Preparation of skin mucus samples for proteomic analysis

The proteins in undiluted salmon skin mucosal fluid were digested in-solution [23]. Aliquots (10 µg total protein/ sample) were dried by SpeedVac centrifugation (Thermo Scientific, Bremen, Germany) and re-dissolved in 100 µL reaction buffer (50 mM NH_4HCO_3). The proteins were reduced with 5 µL 200 mM dithiothreitol (Millipore-Sigma; St. Louis, MO, USA) in reaction buffer for 1 h at 30°C and subsequently alkylated with 15 µL 200 mM iodoacetamide in reaction buffer for 1 h at room temperature in the dark. After dilution with 100 µL reaction buffer, proteins were digested with trypsin (Trypsin Gold mass spectrometry grade, Promega, Madison, WI, USA) at an enzyme/sample ratio of 1:30 at 37°C overnight. The samples were desalted using OMIX C18 10 µL clean-up tips (Agilent Technologies, Santa Clara, CA, USA) in accordance with the manufacturer's instructions and dried by SpeedVac centrifugation. Peptides were re-dissolved in 20 µL 0.1 % (v/ v) formic acid, sonicated for 30 s, centrifuged for 10 min at 13000 × g, transferred to mass spectrometry (MS) vials, and stored at −20°C until analysis.

2.7 Untargeted proteomic analysis by UHPLC-nESI-HRMS

The prepared samples were analyzed using ultra-high pressure liquid chromatography (Dionex Ultimate 3000 UHPLC) coupled via a nano-electrospray ion source (nESI) to a Q-Exactive Hybrid Quadrupole-Orbitrap high-resolution mass spectrometer (HRMS) (Thermo Fisher Scientific, Bremen, Germany) as previously described [23]. Peptide solution (5 µL) was injected onto a µ-precolumn (Acclaim PepMap100, C18, 5 µm resin, 100Å, 300 µm i.d. x 5 mm; Thermo Fisher Scientific) and eluted in back-flush mode onto the analytical column (Acclaim PepMap100, C18, 3 µm resin, 100 Å, 75 µm i.d. x 5 cm, nanoViper; Thermo Scientific). Chromatographic separation was achieved using a binary gradient from 3% to 50% of acetonitrile in water (both containing 0.1% formic acid) for 60 minutes, with 0.3 µL/min flow rate. Peptides were analyzed in positive ion mode applying high-energy collisional dissociation (HCD) fragmentation with normalized collision energy set to 28, acquiring one MS survey scan in the mass range of *m/z* 300–2000, followed by MS/MS of the ten most intense ions.

MS data were analyzed with Proteome Discoverer 1.0 software (Thermo Scientific) using the SEQUEST search engine (La Jolla, CA, USA) with the criteria enzyme name (trypsin), missed cleavage sites (2), precursor peptide mass tolerance (10 ppm), fragment mass tolerance (0.06 Da), fixed modifications of cysteine (carbamidomethyl) and variable modification (oxidation of methionine), and compared to entries for Atlantic salmon in the UNIPROT-database.

2.8 Data processing and visualization of proteomics data

The salmon skin mucus proteomics data were processed using Scaffold Viewer, version 4.8.9. (Proteome Software Inc, Portland, OR, USA). Data analysis was performed using a protein probability threshold of 99.0% minimum with at least one identified peptides per protein and a peptide probability threshold of 95%. The normalized total ion count (TIC) for each protein per sample was used semi-quantitatively to compare protein abundances. Normalization was performed by adjusting the TIC sum for all detected proteins within a sample to the average of the TIC sums of all samples in the study. Venn analysis was performed for the comparison of treatment groups.

PEAKS Studio Viewer version 8.5 (Bioinformatics Solutions, Waterloo, ON, Canada) was applied for result visualization based on normalized TIC filtered with a false discovery rate (FDR) of 1%, one unique peptide identified, and a mass error tolerance of 10 ppm. The filtering parameters for peptides were set to Quality ≥ 5, Intensity ≥ 5E6, 2 ≥ Charge ≥ 5. Protein significance was set to ≥ 20, and Welch's ANOVA was used as significance method. One sample in the Cl_0-E17 group was defined as a reference point for generating a protein profile heatmap.

2.9 Characterization of proteins by biological functions

Functional analysis of proteins that were differentially expressed in the skin mucus of chloramine-treated and

control fish was performed using Gene Ontology (GO) (http://www.geneontology.org) employing the Panther classification system (http://www.pantherdb.org/) [24] after converting the protein names to the correct import format by using the UniProt tool (https://ebi14.uniprot.org/uploadlists/). The introduction of GO removed redundancies and allowed connection with hierarchically clustered biological processes, which are allotted to specific identification numbers. The frequencies of the detected biological processes were compared between treatment groups.

2.10 Untargeted metabolomics analysis using LC-HRMS

Skin mucus samples were thawed at on ice and transferred to chromatography vials [22]. Quality control samples (QC) were prepared by pooling 5 µL aliquots from 33 samples. This number was a result of the limited amount of available mucus, which was very low (i.e., <20 µL) for several samples. However, the QC sample contained aliquots from all groups. The pooled QC sample was run periodically throughout the whole LC-HRMS experiment. Samples were placed randomly in the autosampler tray of a Vanquish Horizon UHPLC (Thermo Scientific), which was thermostatted to 10° C. The UHPLC was interfaced with a Q-Exactive Hybrid Quadrupole-Orbitrap HRMS equipped with a heated electrospray interface.

Separation was achieved by hydrophilic interaction chromatography (HILIC) using a zwitterionic SeQuant ZIC-pHILIC column (Merck, Kenilworth, NJ, USA; 150 × 4.6 mm, 5 µm). The mobile phases consisted of 20 mM ammonium carbonate (A, pH 8.3) and acetonitrile (B). The column was eluted isocratically for 1 min using 80% B, followed by linear gradient elution to 20% B in 29 min. After flushing the column with 8% B, the mobile phase composition was returned to the starting conditions and equilibrated for 9 min. The HRMS was run in positive and negative ion full-scan mode using fast polarity switching in the mass range *m/z* 58–870. The mass resolution was set to 70,000 at *m/z* 200. The spray voltage was 2.8 and 3.2 kV (positive and negative mode, respectively), the transfer capillary temperature was 280 °C, and the sheath and auxiliary gas flow rates were 35 and 10 units, respectively. Xcalibur software version 2.3 was used for instrument control.

2.11 Pre-processing of metabolomics data and quality control

The raw data were converted to ABF format and then processed using MS-DIAL v3.5 [25]. Data in negative and positive mode raw files were processed separately, applying specific parameters (Supplementary Table 1). The resulting data matrix contained retention time and mass-to-charge ratio (RT, *m/z*) and the areas of detected metabolic features. We then evaluated the data to identify drift, which is in LC-HRMS experiments typically corrected by modeling a cubic spline-regression based on the QC samples, and then correcting the abundances of all samples by reversing the modeled effect of the drift. This process was developed independently for each feature. We calculated the non-parametric alternatives of the relative standard deviation and D-ratio [26] with a cut off of 0.2 and 0.4, respectively. In case of missing values, imputation was done using the Random Forest algorithm. All calculations were performed using the notame (v0.0.900) package in R [27]. Exploratory multivariate analyses by principal component analysis (PCA) of the log-transformed and Pareto-scaled values was performed in SIMCA-P (version 15; Umetrics AB, Umeå, Sweden) to visualize the total variation of the metabolite profiles.

2.12 Feature clustering of the metabolomics data

In untargeted metabolomics studies, several features can originate from the same metabolite, and thus, they are assumed to be highly correlated. Therefore, we have implemented the feature clustering-algorithm included in the notame package in the data processing workflow. The algorithm identifies pairs of correlated features within a specified retention time window and a correlation threshold (0.1 min and 0.90, respectively, for this study). The advantage of this process is not only that it facilitates the identification of correlated features but also generates cleaner datasets, reducing the amount of noise that can disturb the subsequent multivariate analysis.

2.13 Statistical analysis of proteomics and metabolomics data, individually and merged

Only proteins that occurred in at least 80% of the samples in one treatment group were included in the subsequent multi-omics statistical analyses. The metabolomics data were restricted to those samples for which proteomics counterparts existed. The processed proteomics and metabolomics datasets were log-transformed and Pareto-scaled in SIMCA-P for multivariate analysis using unsupervised models (PCA) and supervised models (orthogonal partial least-squares-discriminant analysis (OPLS-DA)).

PCA was used for an initial multivariate data analysis with the primary purpose of detecting potential outliers and identify clustering patterns. An OPLS-DA model, which has been shown to be a reliable tool for omics studies [28,29], was built for each comparison of different treatment groups with the aim to identify discriminating proteins or metabolites. The advantage of using OPLS-DA is its capability to decompose the data into "predictive" information related to the response of Y (in our study: exposure to chloramine) and "orthogonal" structured information that is uncorrelated to the response, and that could be associated to factors such as technical or biological

variation, i.e., time [30]. Thus, two types of variable importance-in-the-projection (VIP) values that are relevant for group discrimination were considered, predictive and orthogonal, which are related to each type of latent variables that comprise the model and aid in the interpretation. In these discriminant analyses, the default seven-round cross-validation in the SIMCA software package was applied. The cross-validation analysis of variance (CV-ANOVA) was calculated to assess the reliability of the generated models.

The interpretative power was improved by building S-plots for single OPLS-DA models and shared-and-unique structures (SUS)-plots for combinations of two different OPLS-DA models containing a similar reference group (i.e., model 1: Cl_0-E17 vs. Cl_0-R21 and model 2: Cl_{60}-E17 vs. Cl_{60}-R21), using the p(corr) (a vector representing the correlation, hence the reliability, to chloramine exposure (Y)). Thus, the SUS-plots facilitated the extraction of relevant proteins or metabolites related to a specific model, allowing the identification of shared features between both models in either a similar or an inverse trend. For such a purpose, we set a relatively strict cut-off of p(corr) ≥ 0.75 for the specific features and ≥ 0.5 for the shared features. In the S-plots, we considered only values fulfilling the requirement $p < 0.05$, p(corr) ≥ 0.8, and VIP ≥ 1 as relevant.

OPLS-DA models, S-plots, and SUS-plots were first generated individually for the proteomics and metabolomics data, resulting in the identification of non-treatment related features that were removed from the data sets. Subsequently, the proteomics and metabolomics were merged, and new OPLS-DA models, S-plots, and SUS-plots for the comparison of different treatment groups were built.

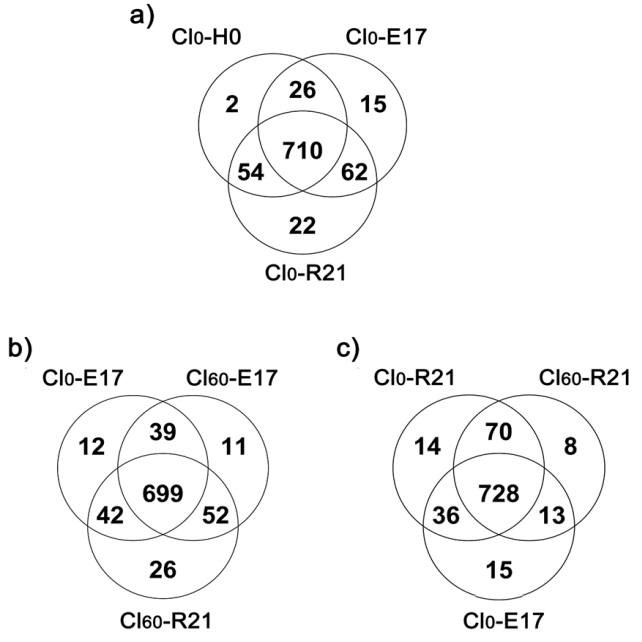

Figure 2 | Comparison of protein occurrences between the groups using Venn diagrams for a) Cl_0-E17, Cl_0-R21, and Cl_0-H0; b) c) Cl_0-E17, Cl_{60}-E17, and Cl_0-R21; c) Cl_0-R21, Cl_{60}-R21, and Cl_0-E17.

3. Results

3.1 Effects of chloramine treatment on the skin mucus proteome of Atlantic salmon

Untargeted proteomic analysis of the skin mucus samples from chloramine-exposed and untreated fish resulted in the identification of in total 895 proteins in the five treatment groups (Cl_0-H0, Cl_0-E17, Cl_{60}-E17, Cl_0-R21, Cl_{60}-R21) with the chosen probability thresholds. One sample in each of the groups Cl_0-H0, Cl_0-E17, and Cl_{60}-E17 had to be excluded from the data set because of the lack of detected proteins. Comparison of protein occurrences between the groups by Venn analysis showed that differences originated mainly from the time spent in the experimental tanks, as demonstrated for the three untreated control groups (Figure 2a). Together, Cl_0-E17 and Cl_0-R21 differed by 99 proteins from Cl_0-H0, whereas only 37 proteins separated the controls at R21 and E17 so that the latter was used as the baseline for treatment comparisons. After exposure to Cl_{60} for 17 days, 63 proteins were identified that were not detected in the untreated control Cl_0-E17. Moreover, 52 of these proteins were also present in the mucus of the treated fish after the recovery period at R21 (Figure 2b). However, when time-dependent changes were considered as deducible from the comparison of Cl_0-E17 to Cl_0-R21, the samples of treated fish differed with eight proteins from the controls at R21 (Figure 2c).

Visualization of the changes in a heatmap showed 58 representative protein groups containing homologous sets, and groups with similar expression trend were clustered together (Supplementary Figure 1). Generally, relative protein abundances were lower at H0 than at E17 and R21, showing a time-dependent trend in the occurrence of most proteins, comparable to the result of the Venn analysis. Examples for this ratio are rab GDP-dissociation inhibitor ((A0A1S3SGW5), heat shock protein 70 (A0A1S3RMM7), and 14-3-3 protein beta/alpha (B5XDE4) (Figure 3). However, a considerable number of proteins were less prevalent at study end, e.g., histone 1 (B9ENS2), betaine-homocysteine methyltransferase (B5DGE7), and sciellin (A0A1S3NV14). Interestingly, some proteins were up- or down-regulated in the skin mucus of chloramine-treated fish at both E17 and R21 as discernable in their group profiles (Figure 3). Up-regulation from Cl_{60} exposure was observed for, among others, glycine-rich cell wall structural protein (A0A1SNVZ3) and thymosin beta-a (C1BXJ6), whereas up-regulation was found for profilin (B5X5I8), glutathione-S-transferase 3 (B5X779), and hemopexin (A0A1S3MVQ2). Several proteins showed differences in expression levels only for Cl_{60}-R21. Up-regulated proteins included, e.g., serotransferrin (B5X2B3) and down-regulated, e.g., peptidyl-prolyl isomerase (C0H7R0).

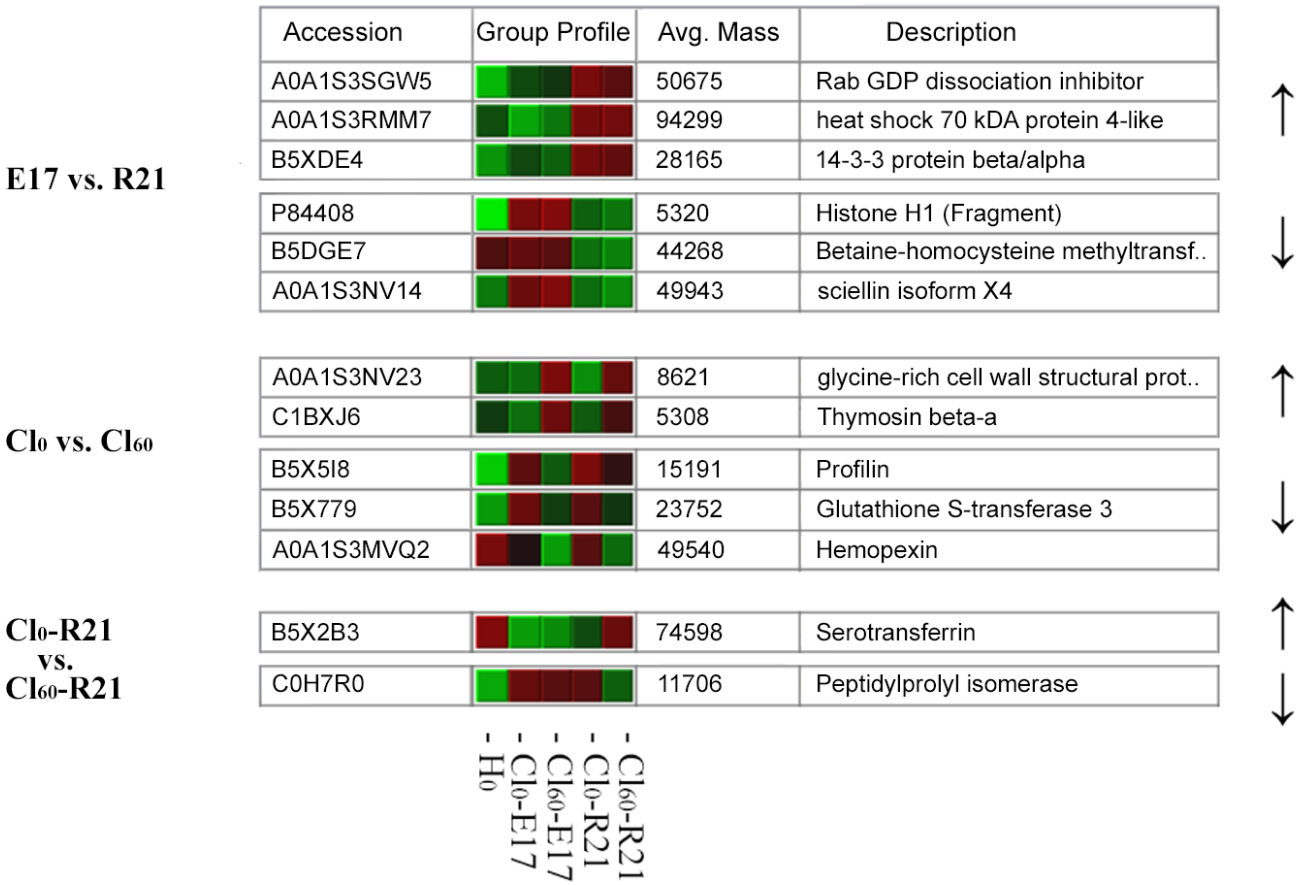

Figure 3 | Group profiles of protein abundances extracted from the proteomic heatmap comparing protein up-and down regulations that are time-dependent (E17 vs. R21), treatment-dependent (Cl_0 vs. Cl_{60}), or relevant at study end (Cl_0-R21 vs. Cl_{60}-R21). The color codes indicate the relative signal strength of the protein in a sample relative to all measured proteins in the same sample and are expressed on a scale of 4 (light red) to -4 (light green) with one of the Cl_0-E17 samples as the reference point. Red color means that the protein was measured with high relative signal strength and green color means that relative signal strength was low compared to the reference sample. Arrows indicate direction of change.

3.2 Effects of chloramine treatment on the skin mucus metabolome of Atlantic salmon

Pre-processing of the raw data from the mucus samples from chloramine-exposed and untreated fish in the five treatment groups (Cl_0-H0, Cl_0-E17, Cl_{60}-E17, Cl_0-R21, Cl_{60}-R21) provided 4534 features from both positive and negative mode. Removal of features with ≥20% CV in the QCs and present in less than 80% of samples of one group resulted in a data matrix containing 3842 metabolic features that were imputated, in case of missing values, and normalized in MS-DIAL. PCA was performed in SIMCA for evaluating metabolite variations. The first model included the QC samples and technical blanks in order to compare instrumental variation and biological variation and to identify possible outliers. The QC samples clustered closely in the center, whereas the blanks of the scores plot confirming the absence of technical bias (Figure 4a). The QC samples were removed from the data set, and a new PCA was performed. It showed that the variation in the metabolite profiles was mostly related to changes in the composition over time and not to exposure to chloramine. The metabolite composition at H0 was markedly different from that at E17 and R21 (Figure 4b).

3.3 Statistical analysis of proteomics and metabolomics data after chloramine exposure (E17)

After quality assessment and restriction of the data set to proteins that occurred in at least 80 % of the samples in a treatment group, 522 proteins were submitted to further analysis (Supplementary Table 2). The metabolomics data set was reduced to samples with existing proteomics data, pre-processed in MS-DIAL, and quality-assessed using the notame package. We detected 1115 features in the negative mode and 2373 in the positive. After data evaluation, 4% of the features in the negative mode were discarded due to a low-detection rate and 19% due to low quality (RSD and D-ratio), whereas in the positive mode, 31% of the features were discarded due to low quality. A drift in the signal intensity was detected for 99% of the features in the negative

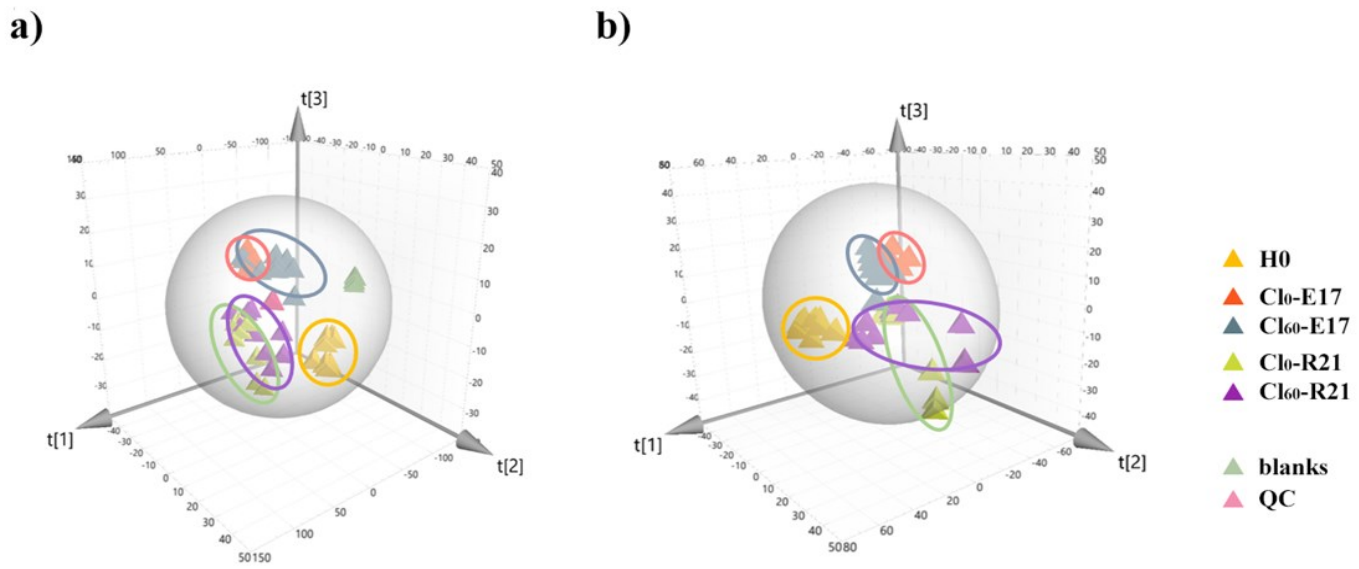

Figure 4 | 3-D scores plot from (Pareto-scaled) principal component analysis (PCA) of metabolic features in skin mucus obtained from a) chloramine-treated salmon and their controls including quality control samples and technical blanks b) chloramine-treated salmon and their controls. H0 = pre-exposure, Cl_0 = control fish, Cl_{60} = chloramine-exposed fish;; E17 = end of 17-day exposure period; R21 = end of 21-day recovery period.

intensity was detected for 99% of the features in the negative and 100% in the positive mode. The drift was corrected through modeling with cubic spline-regression based on the QC samples. When looking for clusters among the samples, we observed 554 connections in the negative mode and 1613 in the positive mode. In total, we created 338 clusters of two or more features, leaving our final dataset with 1889 features. Prior to the integration of the two omics sets, explorative PCA models were built to identify potential outliers (data not shown).

The curated data were used to build OPLS-DA models in SIMCA for the comparison of Cl_0-E17 vs. Cl_{60}-E17, aiming to identify potential differences in the proteomics and in the metabolomics data. However, the respective models did not show significant separation between the treatment groups on day E17 (data not shown).

3.4 Statistical analysis of proteome and metabolome changes in the recovery period (E17 vs. R21)

We built separate OPLS-DA models for the discovery of changes in the proteome and metabolome when comparing the groups Cl_0-E17 vs. Cl_0-R21 and Cl_{60}-E17 vs. Cl_{60}-R21. The analysis confirmed the previously detected dependency of protein expression and metabolite occurrence on the duration of the study. The models generated for Cl_0-E17 vs. Cl_0-R21 were able to discriminate between the two sampling time points and were significant after cross-validation (proteomics model: LV:1+0; R_2X:0.421; R_2Y:0.935; Q_2:0.816; CV-ANOVA = 0.0144373 and metabolomics model: LV:1+1; R_2X:0.582; R_2Y:0.995; Q_2:0.93, CV-ANOVA = 0.00899519). The same was true for the chloramine-exposed groups Cl_{60}-E17 vs. Cl_{60}-R21 (proteomics model: LV:1+0; R_2X:0.38; R_2Y:0.921; Q_2:0.837; CV-ANOVA = 0.000713824 and metabolomics model: LV:1+1; R_2X:0.443; R_2Y:0.985; Q_2:0.77; CV-ANOVA = 0.0404403).

SUS-plots for the proteomics and metabolomics data were generated by combining the respective two OPLS-DA models for Cl_0-E17 vs. Cl_0-R21 or Cl_{60}-E17 vs. Cl_{60}-R21. The plots provided graphical presentations of the proteins and metabolites that were responsible for the unique changes in both group comparisons, and for shared changes in both the chloramine-treated and control groups, extending in either the same or the opposite direction (Supplementary Figure 2). In the proteomic SUS-plot, we identified 165 proteins that changed in the same direction in both groups over time. Since they changed similarly in chloramine-treated and untreated fish, these proteins are probably related to the time spent in the experiment or aging of the fish, confirming the preceding analyses. The implicated proteins were eliminated from the data set to reduce the impact of aging on the outcome. In the metabolomics SUS-plot, 301 metabolites were identified that changed in the same direction in both treatment groups, which could be attributed to the age effect. They were consequently removed from the data set.

3.5 Statistical analysis of proteome and metabolome changes at study end (R21)

OPLS-DA models for Cl_0-R21 vs. Cl_{60}-R21 were created for both the proteomics and metabolomics data. They were able to discriminate between the chloramine-treated fish and controls and were significant after cross-validation (proteomics model: LV: 1+0; R_2X:0.221; R_2Y:0.913; Q_2:0.69; CV-ANOVA = 0.00922 and metabolomics model: LV: 1+2; R_2X:0.492; R_2Y:0.993; Q_2: 0.836, CV-ANOVA = 0.0489).

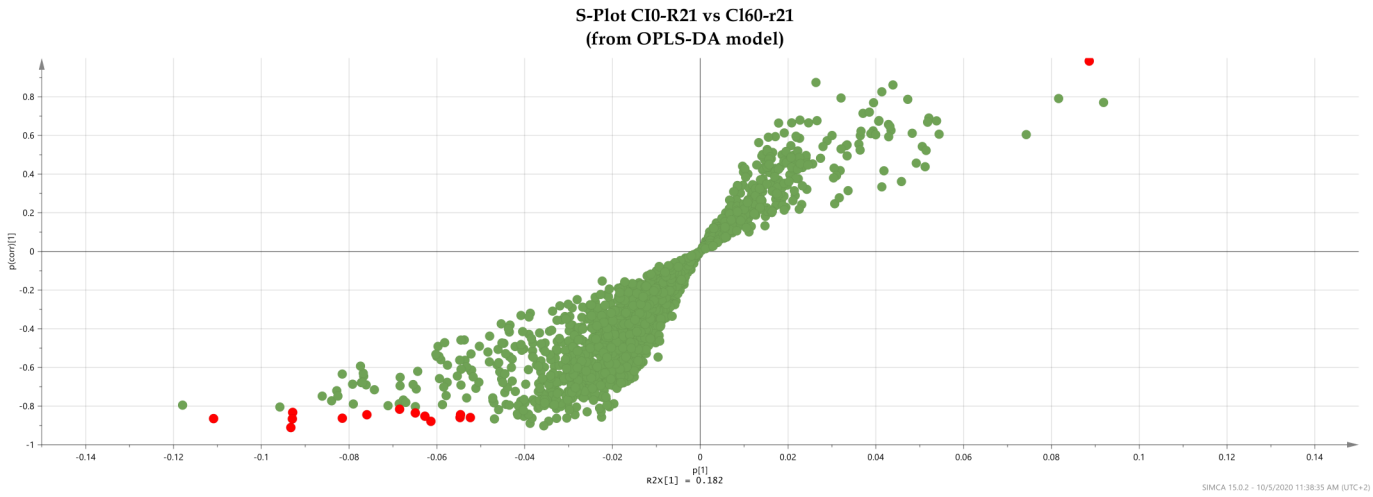

Figure 5 | S-plot from OPLS-DA model comparing proteomic and metabolomic features in Cl_0-R21 vs. Cl_{60}-R21 samples. We set a cut-off $p < 0.05$, $p(corr) \geq 0.8$, and VIP ≥ 1 for selecting a compound as relevant.

3.6 Integration of proteomics and metabolomics data for evaluating changes in the skin mucus from the treatment with chloramine (E17; E17 vs. R21; R21)

The curated proteomic and metabolomics data were used to create a merged omics dataset. New OPLS-DA models were built for group comparisons at E17, E17 vs. R21, and R21. The model for Cl_0-E17 vs. Cl_{60}-E17 indicated separation between the two groups but was not significant (data not shown).

The two models for the comparison of Cl_0-E17 vs. Cl_0-R21 and Cl_{60}-E17 vs. Cl_{60}-R21 were capable to discriminate between samples from day E17 and R21 (Cl_0-E17 vs. Cl_0-R21: LV: 1+0; R_2X:0.258; R_2Y:0.972; Q_2: 0.739; CV-ANOVA = 0.03464; Cl_{60}-E17 vs. Cl_{60}-R21: LV: 1+0; R_2X:0.182; R_2Y:0.931; Q_2: 0.55; CV-ANOVA = 0.0411). We extracted the most relevant features using S-plots. In the plot for the control groups, 24 proteins and 11 metabolites were the most discriminant features separating between E17 and R21, whereas in the plot for the chloramine-treated groups, 12 proteins and 8 metabolites were responsible for the differentiation (Supplementary Table 3). Interestingly, none of the features overlapped between the groups.

The model comparing chloramine-treated and control fish at R21 was able to discriminate significantly between Cl_0-R21 vs. Cl_{60}-R21 (LV: 1+2; R_2X:0.478; R_2Y:0.997; Q_2: 0.869; CV-ANOVA = 0.02904). We extracted the most relevant features causing the separation by using an S-plot (Figure 5), which made it possible to identify 11 specific proteins and four metabolites (Table 2).

3.7 Assignment of proteins to biological processes

Relevant proteins contributing significantly to treatment group separation in the comparisons of Cl_0-E17 vs. Cl_0-R21, Cl_{60}-E17 vs. Cl_{60}-R21, and Cl_0-E21 vs. Cl_{60}-R21 were evaluated for their affiliation to specific biological processes using GO (Table 2; Supplementary Table 3). Accordingly, differences in the untreated controls at E17 and R21 resulted mainly from proteins involved in the "cell process" and "metabolic process" (Figure 6a). The same applied for samples from chloramine-treated fish at E17 and R21 (Figure 6b), confirming the considerable influence of the experiment duration and fish age on protein expression and occurrence in the skin mucus. Comparison of Cl_0-E21 vs. Cl_{60}-R21 at the study end indicated a notable contribution of proteins connected to "biological regulation" and "cellular component organization or biogenesis" to the observed differences (Figure 6c), which might be attributable to the chloramine treatment.

4. Discussion

The chlorination of Norwegian rivers and lakes at low concentrations is currently considered as a promising alternative to the use of toxins in the efforts to fight infection of wild salmon with the fluke Gyrodactylus salaris [12]. First trials in restricted areas have shown that chlorine water concentrations of up to 50 µg/L effectively removed the parasites from the fish without causing apparent toxic effects [10]. Chloramine has been found to be a practicable precursor of active chlorine that is quickly released under contact with water. However, before this method can be applied as a large-scale measure for the recovery of watercourses, consequences for the salmon have to be studied in more detail. In this context, the present study contributes to the evaluation of chloramine's suitability as a selective and gentle agent in the fight against the salmon fluke.

Consequences of chloramine exposure for the incidence of oxidative stress biomarkers in the liver of rainbow trout (Oncorhynchus mykiss), brown trout (Salmo trutta), and grayling (Thymallus thymallus) have been analyzed previously without finding significant changes, although the fish had been treated with concentrations as high as 9 mg/L [9,31]. Another study on rainbow trout using the same high

Table 2 | Most discriminant proteomic and metabolomic features separating Cl_0-R21 vs. Cl_{60}-R21, as identified by S-plot analysis. *UniProt, with ending _SALSA; #by proteomic analysis; ¤maximum in treatment group Cl_{60}-R21; analysis with HILIC-HRMS/MS

Accession number*	Protein name	Molecular weight [kDa]	Sequence coverage#¤ [%]	Identification probability¤ [%]	vs. Cl_0
B5X6W1	Calpain small subunit 1	24.56	42.6	100	↓
B5X1Q8	Leukocyte elastase inhibitor	42.88	6.6	100	↓
B5DGU3	Proteasome subunit alpha type	27.36	4.1	100	↓
C0H9W4	Thimet oligopeptidase	77.74	14.9	100	↓
B5RI51	Barrier-to-autointegration factor	10.86	12.4	100	↓
B5XFL6	Plastin-2	20.44	31.0	100	↓
C7C4W8	L-plastin (Fragment)	14.54	18.2	100	↓
B9EPG1	Thioredoxin	12.18	22.2	99.3	↓
B5X8U9	Probable thiopurine S-methyltransferase	26.68	6.0	99.8	↓
RBM8A	RNA-binding protein 8A	19.89	10.9	98.5	↓
B5DG91	Apoptosis-assoc. speck-like protein contain. a CARD	21.99	6.1	95.8	↓

Metabolite ID number*	Ion mode	Retention time	Molecular weight (*m/z*)	vs. Cl_0
174_0404a19_49	neg.	19.49	174.040	↓
221_0663a8_825	neg.	8.83	221.066	↑
226_0837a10_694	neg.	10.69	226.084	↓
477_1712a10_66	pos.	10.66	477.171	↓

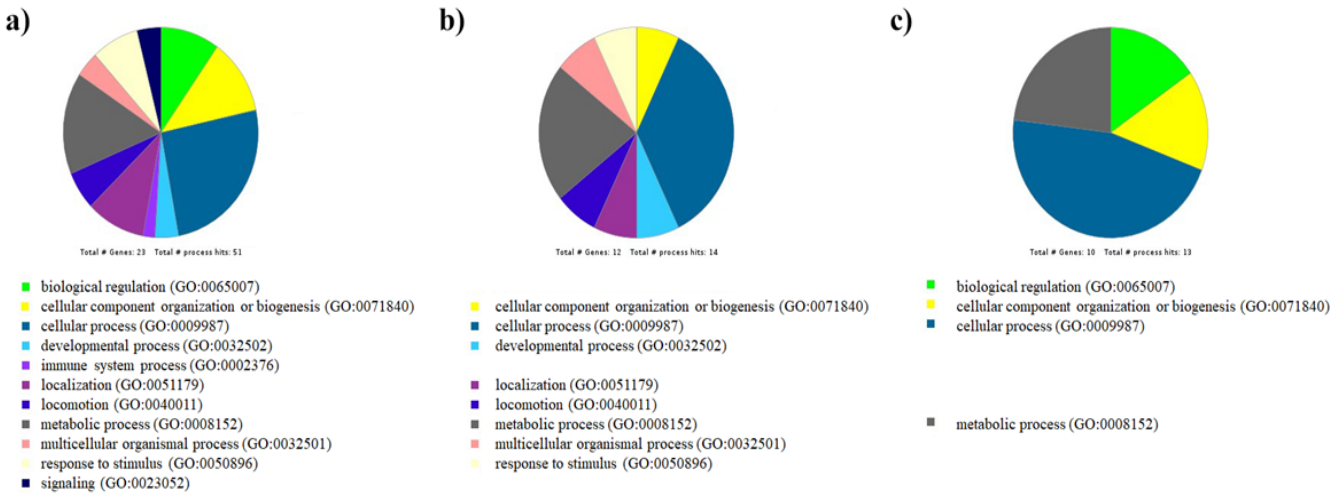

Figure 6 | Relevant biological processes (determined using Gene Ontology) assigned to the most relevant proteins extracted from the OPLS-DA models comparing a) Cl0-E17 vs. Cl0-R21, b) Cl60-E17 vs. Cl60-R21, and c) Cl0-E21 vs. Cl60-R21.

chloramine concentration did not detect changes in the hemoglobin and hematocrit levels, but registered a small increase in the cardiac output, facilitating increased O2 uptake [32]. In contrast, coho salmon (Oncorhynchus kisutch) exposed to 30 µl/L total residual chlorine in municipal wastewater mixed into seawater showed signs of sublethal stress as demonstrated by reduced hemoglobin and hematocrit concentrations [14]. The existing information on the effects of chlorine and chloramine on fish is thus relatively scarce and inconclusive, so that new knowledge is needed to better understand mechanisms of the physiological adaptation of salmon to the treatment.

The sampling of blood or liver samples from fish is laborious, and for the fish, stressful or deadly. Therefore, skin mucus has come up as an alternative source for health monitoring, since its collection is minimally invasive, simple, and can be performed several times on the same fish during long-term experiments [23,33]. The composition of fish skin mucus has been found to be considerably influenced by exposure to internal or external stress factors [34]. Analysis of the proteins and metabolites in the mucus can thus give valuable information on triggered deviations from the normal physiological state.

The combination of proteomics and metabolomics is a novel, comprehensive approach for the characterization of changes in the expression fingerprint of fish, which can help to identify main underlying processes and potentially identify solutions to improve viability. Recent studies have shown an increase in metabolomics and proteomics techniques for different applications in aquaculture [19,35–37]. However, due to the complexity of the data generated, it requires comprehensive statistical methods and visual interpretation to extract biological information. Traditionally, omics data are comprised of thousands of variables derived from relatively low numbers of samples, which makes subsequent processing with traditional univariate methods problematic due to the possible generation of false positives. In contrast, multivariate analysis has proven its applicability to handle such extensive and multidimensional datasets. In particular, OPLS-DA modeling is useful for interpreting complex relationships between different groups of samples. This statistical method explains their correlated variability but considers at the same time also the orthogonal-structured (non-correlated) variation between them.

To our knowledge, this is the first multi-omics approach aimed to study combined changes in the skin mucus proteome and metabolome of salmon that have been exposed to waterborne substances. We have used comprehensive, integrated omics analysis to reveal potential responses from a 17-days treatment with (mono)chloramine at a concentration of 60 µg/L, which was two- to threefold above the concentration that is intended to be applied in the treatment of Norwegian rivers. In this way, the importance of potential findings could be evaluated against the built-in safety margin.

The results from the proteomic and metabolomic measurements were first assessed individually before the data were joined for a combined statistical modelling. The total number of detected salmon skin mucus proteins was in the same range as in a previous study using the same sampling method [21]. The initial data exploration showed that differences between the protein profiles of the experimental groups were small and mostly related to the "age-effect," i.e., the duration of the study. This was particularly relevant for proteins that have been found to occur with high abundances in salmon skin mucus in a previous study such as, e.g., 14-3-3 protein (B5X4L8), enolase (B5DGQ7), malate dehydrogenase (B5XBK0), heat shock protein 70 (A0A1S3RMM7), and tubulin (C0HBL4) [21]. The few proteins separating Cl_{60}-treated and control fish after the exposure (E17) and the recovery (R21) period included glycogenin-1 (B5XCR2), histone H3 (B5DG71), grancalcin (B5X3Y4), spectrin alpha (C0PUV6), thymosin beta-a (C1BXJ6), glutathione-S-transferase 3 (B5X779) and NEDD8-conjugating enzyme (C0HBK6), which are, respectively, involved in carbohydrate metabolism, DNA structure, muscle activity, and protein modifications. Their association, mainly with metabolic processes, may indicate activation by chloramine exposure, potentially in connection with the increased O_2 blood levels [32]. Interestingly, typical immune response proteins appeared not to be affected by the Cl_{60}-treatment, confirming the relatively good toleranceof low chloramine concentrations in salmon [10,12]

The metabolic signatures in the skin mucus of chloramine-exposed and untreated salmon did not differ significantly, as demonstrated by PCA analysis. However, in accordance with the observations made for the mucus proteome, the metabolite profiles showed a clear age-dependent trend. Moreover, an indication for separation between treated and control fish was visible at E21 after the recovery period, meaning that exposure to chloramine might lead to the setting of a slightly different physiological base level.

When we subsequently combined the proteomic and metabolomic datasets, the integrated analysis allowed a more differentiated evaluation of the observed trends. Again, we identified shared features among treated and non-treated fish across time. Assuming that they were related to aging, and thus could be confounding factors associated incorrectly with chloramine exposure, we created our final models without this structured variation. For the identification of the relevant features, we compared the changes between the days E17 and R21 for Cl_0 and Cl_{60} independently. Whereas significant differences were not identifiable by univariate analysis, our multivariate models showed that both groups experienced specific changes. The most significant models to achieve the discrimination between E17 and R21 were comprised of only a predictive component without any orthogonal counterpart, indicating that the correlated and the orthogonal variability are merged in order to maximize the separation between groups, which involves a risk of overfitting. In fact, when we added an orthogonal

component (data not shown), we observed that the models were no longer significant. Significance of the E17 vs. R21-models for the treated and non-treated samples was thus probably caused by merging the variabilities. Nevertheless, the time-related changes are relevant because they reflect the growth and physiological changes of the salmon. Moreover, although the features contributing the most to the age effect in the control group were not in the top list of the chloramine-exposed group, they also appeared as discriminating factors for the latter.

When we made a direct comparison between treated fish and controls at R21, proteinaceous and metabolic features discriminating between the groups were detectable. Several proteins that were present in the skin mucus of the control fish were not found in samples of chloramine-exposed fish and thus characterized the separation. Classification of these proteins, according to GO, showed that they were related to metabolic processes, supporting the above conclusion of the proteomics data. The OPLS-DA for Cl_0-E21 vs. Cl_{60}-R21 was comprised of 1 predictive + 2 orthogonal components, implying a high within-samples variability. The identification of metabolomic features by additional fragmentation experiments was not feasible in the present study, reducing the opportunities for compound annotation. However, the use of a novel processing tool for feature clustering helped us to merge similar metabolomics features, leading to a more compressed dataset and reducing the collinearity between the metabolomics datasets of the different experimental groups. This facilitated the interpretation of the metabolomics part of this study and allowed the group allocation and tentative labeling of several metabolites. Interestingly, the feature 221_0663a8_825 (*m/z* 221.066; negative ion mode), which is up-regulated by chloramine treatment at R21, could be preliminarily identified as D-glycero-L-galacto-octulose. A recent report shows that the synthesis of this sugar may involve an alternative pentose phosphate pathway, and that high levels might contribute favorably to ROS scavenging [38]. Thus, higher octulose production could be a reaction of the salmon to the increase of ROS activity in the water and skin mucus from exposure to chloramine and hydrolysis and breakdown products.

5. Concluding Remarks

The safe use of a low level of chloramine for the control of salmon fluke infections in Norwegian watercourses has been investigated in a controlled exposure study. The combined analysis of the skin mucus proteome and metabolome revealed only insignificant differences between treated and control salmon after 17 days, and minor changes after a 21-day recovery period. These results indicate that the health risk for salmon exposed to chloramine concentrations below 60 µg/L is low.

Acknowledgments:

The authors would like to express their sincere thanks to the late Mr. Trond Håvelsen from the Fish Administration for Drammen city and county (Drammen og Omland Fiskeadministrasjon (DOFA)) for the generous gift of young wild salmon from their fish nurseries. Without your contribution, we could not have carried out this project. We miss you as a congenial, open-minded, and amicable colleague. This study was funded by the Norwegian Environment Agency and additionally, by the Norwegian Veterinary Institute (NVI), the Norwegian Institute for Water Research (NIVA), and the Norwegian Institute for Nature Research (NINA).

Supplementary material:

Supplementary Table 1
Supplementary Table 2
Supplementary Table 3
Supplementary Figure 1
Supplementary Figure 2

References

[1] B.O. Johnsen, Astarte (1978).
[2] B.O. Johnsen, P.I. Møkkelgjerd, A.J. Jensen, NINA Oppdragsmeld. 617 (1999) 1–129.
[3] S. Hytterød, M. Darrud, K. Johansen, S. Larsen, S.N. Mohammad, H. Hansen, The Surveillance Programme for Gyrodactylus Salaris in Atlantic Salmon and Rainbow Trout in Norway 2017, 2018.
[4] T. Mo, in: Diagnosis Control Fish Dis., 2004, p. 18.
[5] DirNat, Handlingsplan (Forslag) Mot Lakseparasitten Gyrodactylus Salaris., 2008.
[6] B.O. Johnsen, Å. Brabrand, P.A. Jansen, H.-C. Teien, G. Bremset, Evaluering Av Bekjempelsesmetoder for Gyrodactylus Salaris. Rapport Fra Ekspertgruppe, 2008.
[7] H.G. Gorchev, G. Ozolins, WHO (2004).
[8] J. From, Progress. Fish-Culturist 42 (1980) 85–86.
[9] G.L. Bullock, R.L. Herman, C. Waggy, J. Aquat. Anim. Health (1991).
[10] M.A. Thorburn, R.D. Moccia, J. Aquat. Anim. Health (1993).
[11] A.G. Hagen, S. Hytterød, K. Olstad, J. Fish Dis. (2014).
[12] A.G. Hagen, S. Hytterød, K. Olstad, Ø. Aaberg, M. Darrud, T.H. Holter, J. Svendsen, T.A. Mo, C. Escudero-Oñate, E. Martinez Francés, M.C. Gjessing, Forsøksbehandling Med Monokloramin Mot Gyrodactylus Salaris i Elva Glitra, 2018.
[13] T.S. Rao, Y. V. Nancharaiah, K.V.K. Nair, Biofouling (1998).
[14] J. Singleton, Ambient Water Quality Criteria for Chlorine, 1989.
[15] J.A. Buckley, C.M. Whitmore, R.I. Matsuda, J.FISH.RES.BOARD CANADA (1976).
[16] Effekter På Laks (Salmo Salar) Ved Eksponering for Monokloramin, 2019.
[17] F. Provan, L.B. Jensen, K.E. Uleberg, E. Larssen, T. Rajalahti, J. Mullins, A. Obach, J. Fish Dis. (2013).
[18] R. Aebersold, M. Mann, Nature 422 (2003).
[19] D.R. Ekman, D.M. Skelton, J.M. Davis, D.L. Villeneuve, J.E.

Cavallin, A. Schroeder, K.M. Jensen, G.T. Ankley, T.W. Collette, Environ. Sci. Technol. (2015).
[20] F.R. Pinu, D.J. Beale, A.M. Paten, K. Kouremenos, S. Swarup, H.J. Schirra, D. Wishart, Metabolites (2019).
[21] B.B. Misra, C. Langefeld, M. Olivier, L.A. Cox, J. Mol. Endocrinol. (2018).
[22] L. Ivanova, H. Tartor, S. Grove, A.B. Kristoffersen, S. Uhlig, Fishes 3 (2018) 21.
[23] C.K. Fæste, H. Tartor, A. Moen, A.B. Kristoffersen, A.K.S. Dhanasiri, J.H. Anonsen, T. Furmanek, S. Grove, J. Chromatogr. B 1138 (2020) 121965.
[24] H. Mi, A. Muruganujan, D. Ebert, X. Huang, P.D. Thomas, Nucleic Acids Res. 47 (2019) D419–D426.
[25] H. Tsugawa, R. Nakabayashi, T. Mori, Y. Yamada, M. Takahashi, A. Rai, R. Sugiyama, H. Yamamoto, T. Nakaya, M. Yamazaki, R. Kooke, J.A. Bac-Molenaar, N. Oztolan-Erol, J.J.B. Keurentjes, M. Arita, K. Saito, Nat. Methods 16 (2019) 295–298.
[26] D. Broadhurst, R. Goodacre, S.N. Reinke, J. Kuligowski, I.D. Wilson, M.R. Lewis, W.B. Dunn, Metabolomics 14 (2018) 72.
[27] A. Klåvus, M. Kokla, S. Noerman, V.M. Koistinen, M. Tuomainen, I. Zarei, T. Meuronen, M.R. Häkkinen, S. Rummukainen, A.F. Babu, T. Sallinen, O. Kärkkäinen, J. Paananen, D. Broadhurst, C. Brunius, K. Hanhineva, Metabolites (2020).
[28] S. Wiklund, E. Johansson, L. Sjöström, E.J. Mellerowicz, U. Edlund, J.P. Shockcor, J. Gottfries, T. Moritz, J. Trygg, Anal. Chem. 80 (2008) 115–122.
[29] O.D. Rangel-Huerta, A. Gomez-Fernández, M.J. de la Torre-Aguilar, A. Gil, J.L. Perez-Navero, K. Flores-Rojas, P. Martín-Borreguero, M. Gil-Campos, Metabolomics 15 (2019) 99.
[30] H.S. Tapp, E.K. Kemsley, TrAC - Trends Anal. Chem. 28 (2009) 1322–1327.
[31] H. Tkachenko, N. Kurhaluk, J. Grudniewska, Arch. Polish Fish. 21 (2013) 41–51.
[32] M.D. Powell, S.F. Perry, Exp. Biol. Online 4 (1999) 1–59.
[33] I. Sanahuja, L. Fernández-Alacid, S. Sánchez-Nuño, B. Ordóñez-Grande, A. Ibarz, Front. Physiol. 9 (2019).
[34] J. Pérez-Sánchez, G. Terova, P. Simó-Mirabet, S. Rimoldi, O. Folkedal, J.A. Calduch-Giner, R.E. Olsen, A. Sitjà-Bobadilla, Front. Physiol. 8 (2017).
[35] P.M. Rodrigues, T.S. Silva, J. Dias, F. Jessen, J. Proteomics (2012).
[36] J. Cerdà, M. Manchado, Genes Nutr. 8 (2013) 5–17.
[37] S.A.M. Martin, E. Król, Dev. Comp. Immunol. 75 (2017) 86–98.
[38] Q. Zhang, D. Bartels, J. Exp. Bot. 68 (2017) 5689–5694.